

3 kV Monolithic Bidirectional GaN HEMT on Sapphire

Md Tahmidul Alam¹, Swarnav Mukhopadhyay¹, Md Mobinul Haque¹, Shubhra S. Pasayat¹, and Chirag Gupta¹

¹Department of Electrical and Computer Engineering, University of Wisconsin-Madison, WI 53706, USA

Abstract— More than 3 kV breakdown voltage was demonstrated in monolithic bidirectional GaN HEMTs for the first time having potential applications in 1200V or 1700V-class novel power converters. The on resistance of the fabricated transistors was $\sim 20 \Omega \cdot \text{mm}$ or $\sim 11 \text{ m}\Omega \cdot \text{cm}^2$. Breakdown voltage was optimized by utilizing two field plates in either side of the transistor and optimizing their geometry. Shorter first field plate lengths ($\leq 2 \mu\text{m}$) resulted in higher breakdown voltage and the possible reason for this was discussed. The transistors had a steep subthreshold swing of 92 mV/dec. The on/off ratio was $>10^5$ and it was limited by the tool capacity. The fabricated 3 kV transistor was benchmarked against the state-of-the-art monolithic bidirectional GaN HEMTs in the performance matrices of breakdown voltage – on resistance, that showed crucial progress.

Index Terms— Monolithic Bidirectional GaN HEMT/Switch (MBDS), Wide bandgap Semiconductors, Bidirectional Switch, 2DEG.

I. INTRODUCTION

Efficient and reliable extraction of renewable energy is essential to encounter the anticipated global energy shortage due to the depletion of fossil fuels in a few decades [1]-[3]. However, the extraction, storage and conversion of energy from renewable sources is still very inefficient compared to theoretical limits because of the lack of high-power, efficient and reliable power converters. Some novel power converters with high power density require bidirectional current and bidirectional blocking capability. Matrix converters, multi-level T-type inverter, current source inverter, solid-state circuit breaker etc. are such examples [4]-[8]. Typically, bidirectional functionality is achieved by connecting two unidirectional transistors in anti-series or anti-parallel configuration [9]-[12]. However, these implementations suffer from high on-resistance, high complexity, low reliability and high form-factor due to high device count (four) and internal contacts. Monolithic bidirectional GaN Transistors / Switches (MBDS) can achieve bidirectional current or blocking capability with a single device hence can potentially mitigate these challenges [13]-[16].

There are several reports on the structure and operation [17],[18], gate-control schemes [19],[20] and substrate termination [21] of monolithic bidirectional GaN HEMTs.

One of our previous works demonstrated 1360V GaN MBDS¹ with a qualitative design guide for breakdown voltage optimization with field plates [22]. However, there is no demonstration of >2 kV breakdown voltage GaN MBDS- which is essential to make 1200 V-class and 1700 V-class power converters. In this work, we report 3 kV (measurement limit of the tool = 3 kV) GaN MBDS for the first time with low on-resistance (R_{ON}) of $\sim 20 \Omega \cdot \text{mm}$ ($11 \text{ m}\Omega \cdot \text{cm}^2$) on sapphire substrate. We utilized and optimized two field plates to maximize the breakdown voltage by electric field management. This work has been benchmarked against the state-of-the art monolithic bidirectional GaN HEMTs, indicating crucial advance.

Conventionally, normally-off transistors are preferred than normally-on transistors in power converters due to the ability of normally-off transistors to withstand any accidental damage of the gate driving circuitry. Moreover, normally-off transistors need simpler gate drivers [23], [24]. However, both normally-on and normally off transistors have been commercialized for power electronic applications. Normally-on transistors can be converted to normally-off by cascoding a low-voltage silicon transistor [15],[16], [25]-[28]. In this work, we fabricated normally-on transistors however similar concepts or designs can be applied to normally-off transistors as well for fabrication of high-voltage applications.

II. TRANSISTOR FABRICATION AND MEASUREMENT

The epitaxial structure- 3nm GaN (cap)/ 20nm $\text{Al}_{0.24}\text{Ga}_{0.76}\text{N}$ (barrier) / 0.7nm AlN/ $1 \mu\text{m}$ UID GaN (channel)/ $2 \mu\text{m}$ semi-insulating GaN (Fe doped, $N_{\text{A}} = \sim 5 \times 10^{18} \text{ cm}^{-3}$)/sapphire substrate was grown in MOCVD (Fig. 1). Sapphire was chosen over silicon as the substrate material to allow higher breakdown voltage beyond 2 kV [29]-[32]. The fabrication process started with standard solvent cleaning, subsequent ohmic lithography and metal deposition- Ti/Al/Ni/Au (20/120/30/50) nm. The ohmic metal stacks were then annealed at 900°C for 45 seconds in N_2 environment. After that, a 750nm deep mesa etch was performed to isolate the devices. Afterwards, 200nm thick Ni gates were deposited in a two-phase deposition- in each phase the plane of the sample was inclined at 30° from the horizontal plane to ensure metal coverage in the sidewall. Then, the surface was passivated by a 320nm thick PECVD Si_3N_4 layer. Next, two field plate trenches were etched in the Si_3N_4 layer such that the first and second trench had $\sim 100\text{nm}$ and $\sim 250\text{nm}$ thick Si_3N_4 left from the AlGaIn barrier. Following this, Ni/Au (200/200) nm was deposited as field plate metals on the trenches. Each field plate was connected to the nearest source/ohmic electrode. The field plate lengths (L_{FP1} and L_{FP2}) were varied between $1 \mu\text{m}$ to $3 \mu\text{m}$ to optimize the breakdown voltage. Gate length (L_{G}), gate-drain distance (L_{GD}), gate-source distance

The authors gratefully acknowledge the support of this research from NSF ASCENT (award number ECCS 2328137).

M.T. Alam, S. Mukhopadhyay, M. Haque, S.S. Pasayat, and C. Gupta are with the Department of Electrical and Computer Engineering, University Wisconsin-Madison at Madison, WI 53706, USA (e-mail: malam9@wisc.edu).

(L_{GS}) and width (distance between Mesa edges, Fig. 1(b)) were $2\mu\text{m}$, $40\mu\text{m}$, $2\mu\text{m}$ and $100\mu\text{m}$ respectively. Table-I contains the detailed structural dimensions of the fabricated transistors.

The B1505A (Keysight) source-measurement unit (SMU) was used to perform DC IV, pulsed IV and breakdown voltage measurements. During breakdown measurements the second gate (G_2) was shorted to the “drain” (S_2) and the devices were immersed in Fluorinert FC-40 to ensure air does not breakdown before transistor breakdown.

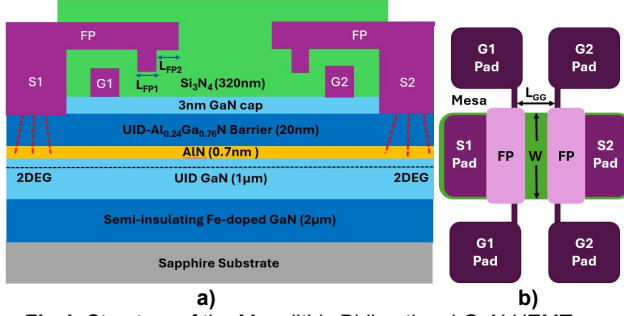


Fig.1. Structure of the Monolithic Bidirectional GaN HEMT. a) Cross-section b) Top view. The source pads were $1\mu\text{m}$ inside the Mesa edge, the field plates covered $2\mu\text{m}$ beyond the Mesa edge.

TABLE I

Parameter	Description	Value
L_G	Gate length	$2\mu\text{m}$
L_{GS}	Gate to source distance	$2\mu\text{m}$
L_{GG}	Gate to gate distance	$40\mu\text{m}$
L_{FP1}	First field plate length	$1\mu\text{m}$ – $3\mu\text{m}$
L_{FP2}	Second field plate length	$1\mu\text{m}$ – $3\mu\text{m}$
L_{GF}	Gate to field plate distance	$1\mu\text{m}$
W	Width	$100\mu\text{m}$
T_{FP1}	Dielectric under first field plate	100 nm
T_{FP2}	Dielectric under second field plate	250 nm

III. RESULTS AND DISCUSSION

A. IV Characteristics

The bidirectional IV characteristics of the MBDS are shown in Fig. 2. For $L_{GG} = 40\mu\text{m}$, the on-resistance was $\sim 20\ \Omega\text{.mm}$ resulting in a specific resistivity of $\sim 11\text{ m}\Omega\text{.cm}^2$. The specific resistivity was found by multiplying the on resistance (R_{ON}) with the total pitch of the channel ($L_{SD} + 2L_T$). TLM (Transfer Length Measurements) was performed to extract the transfer length ($2L_T \sim 7\mu\text{m}$), contact resistance ($R_c \sim 0.9\ \Omega\text{.mm}$) and sheet resistance ($R_{sheet} \sim 350\ \Omega/\square$) of the 2DEG. The extracted value of R_{ON} from IV curves matched closely with the expected R_{ON} from R_c and R_{sheet} . The sheet charge density was $8.35 \times 10^{12}\text{ cm}^{-2}$, and electron mobility was $2010\text{ cm}^2/\text{V.s}$, determined by hall measurements.

The threshold voltage (V_{TH}) was stable -3.25 V in multiple measurements (assuming 1 mA/mm to be the cut-off current) as observed from the transfer characteristics in Fig. 3. The subthreshold swing (SS) was steep 92 mV/dec (between 10^{-4} A/mm to 10^{-5} A/mm), on/off ratio was $>10^5$ and was limited by the tool noise current in the low-current domain. The stable V_{TH} , low SS along with high on/off ratio makes this device suitable for high-frequency operations with low conduction and switching losses.

B. Breakdown Voltage

Fig. 4 depicts the breakdown response of a transistor with 3 kV breakdown voltage. Both the gate-leakage and drain-leakage current was noticeably stable ($I_D \sim 90\ \mu\text{A/mm}$ and $I_G \sim 2\ \mu\text{A/mm}$) and below 1 mA/mm (breakdown limit) up to the tool limit of 3 kV [33]–[35]. The breakdown voltage was 3 kV (tool limit) for most devices with the first field plate length (L_{FP1}) of $\leq 2\ \mu\text{m}$. However, transistors $L_{FP1} > 2\ \mu\text{m}$ exhibited a tendency to have lower breakdown voltage ($< 3\text{ kV}$) as shown in Fig. 5. A possible reason for this trend is that longer total field plate length causes the electric field under the field plates to become stronger. Thus, it results in a high impact ionization rate and causes early transistor breakdown. The detailed mechanism of breakdown is described and justified with TCAD simulations in one of our earlier works [18]. Fig. 6 demonstrates the promising stand of our fabricated MBDS' in the breakdown voltage – on-resistance benchmark compared to the state-of-the-art MBDS'. The reasonable stability of the leakage current and the superior stand in the breakdown voltage – on-resistance benchmark of our fabricated transistors makes them an attractive choice for potential 1700V -class or 1200V -class applications. However, the breakdown field ($\sim 75\text{ V}/\mu\text{m}$) is still much lower than the theoretical critical field ($330\text{ V}/\mu\text{m}$) of GaN. The critical field or breakdown voltage of the transistors may further be increased by optimizing the field plate number and geometry. We are currently working on this optimization and our future works are expected to publish the relevant studies.

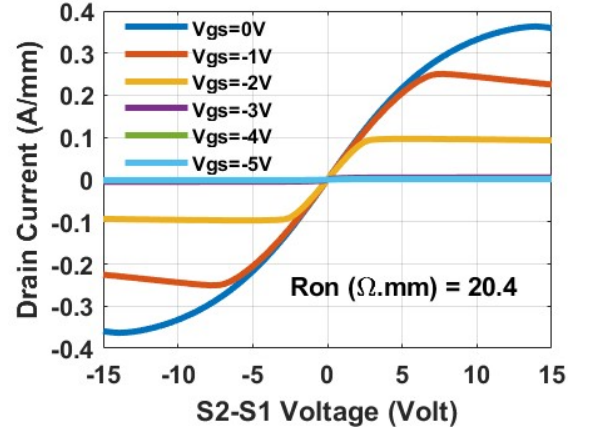


Fig. 2. Bidirectional IV characteristics of the MBDS with $L_{GG} = 40\mu\text{m}$, $L_G = 2\mu\text{m}$, $L_{GS} = 2\mu\text{m}$.

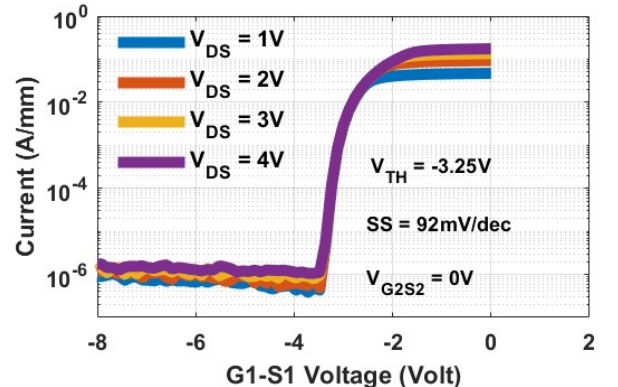


Fig.3. Transfer characteristics of the MBDS showing a steep SS of 92 mV/dec and on/off ratio $\sim 10^5$.

C. Preliminary Dynamic Response

Pulsed IV measurements with 40V off-state switching voltage (limited by tool capacity) was performed, the dynamic R_{ON} was <10% higher than DC R_{ON} at $V_{DS} = 1V$ (Fig. 7) with 100 μ s pulse width. The amount of current collapse was less than 10% compared to DC measurements. In these measurements the second gate (G_2) and “drain” (S_2) were shorted together. Even though the preliminary switching results look promising, the off-state switching voltage should be close to the voltage rating of the application class (~1200V or ~1700V) with <10 μ s pulse width for practical implementations. The 40 V applied bias in this study was due to the tool limit. Our future studies will focus on high voltage switching tests with appropriate tool setup.

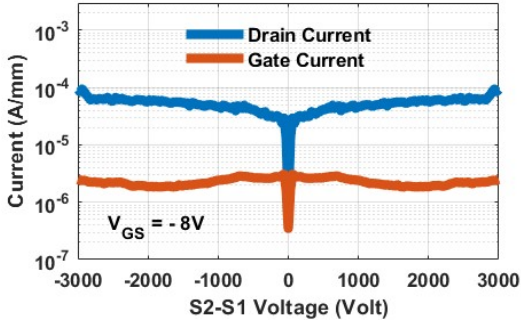


Fig. 4. Breakdown response of an MBDS with field plate 1 and 2 length of 1 μ m and 1.5 μ m respectively.

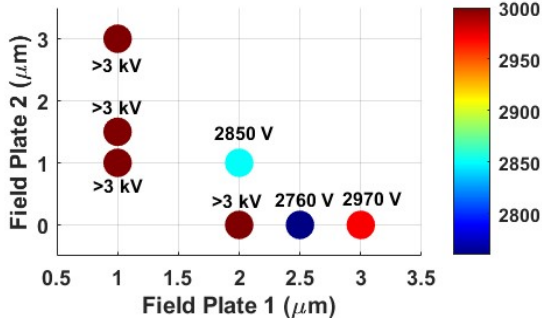


Fig. 5. Breakdown voltage variation with field plate dimensions, transistors with smaller first field plate length had higher breakdown voltage.

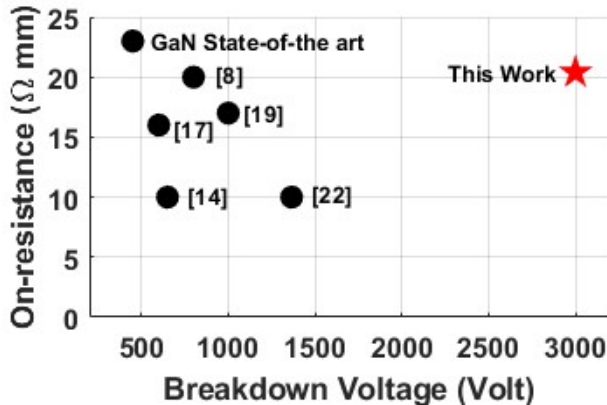


Fig. 6. Standing of our fabricated MBDS with state-of-the-art in breakdown voltage- R_{ON} benchmark.

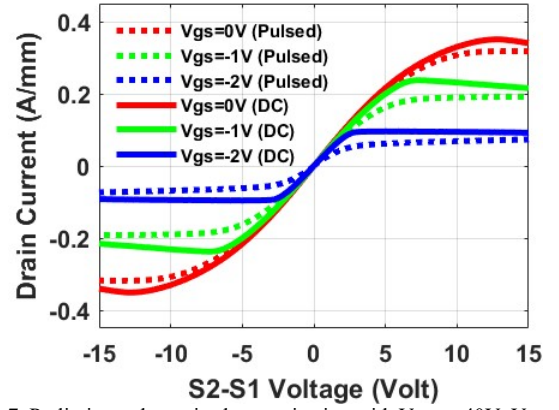


Fig. 7. Preliminary dynamic characterization with $V_{DSQ} = 40V$, $V_{GSQ} = -12V$, pulse width = 100 μ s.

IV. CONCLUSION

Monolithic bidirectional GaN HEMTs with greater than 3 kV (limited by tool capacity) breakdown voltage was demonstrated for the first time for potential applications in 1200V-class or 1700V-class power converters. The breakdown voltage was optimized by utilizing two field plates with varying lengths. The first field plate lengths of $\leq 2\mu$ m resulted in higher breakdown voltage, the possible physics behind this was explained. For 3 kV breakdown voltage the on-resistance was low, $\sim 20 \Omega \cdot \text{mm}$ (11 m $\Omega \cdot \text{cm}^2$). In breakdown voltage – on resistance benchmark against the state-of-the-art monolithic bidirectional GaN HEMTs, this work shows significant progress.

REFERENCES

- [1] N. Abas, A. Kalair, and N. Khan, “Review of fossil fuels and future energy technologies,” *Futures*, vol. 69, pp. 31–49, May 2015, doi: 10.1016/j.futures.2015.03.003.
- [2] S. Shafiee and E. Topal, “When will fossil fuel reserves be diminished?,” *Energy Policy*, vol. 37, no. 1, pp. 181–189, Jan. 2009, doi: 10.1016/j.enpol.2008.08.016.
- [3] I. Capellán-Pérez, M. Mediavilla, C. de Castro, Ó. Carpintero, and L. J. Miguel, “Fossil fuel depletion and socio-economic scenarios: An integrated approach,” *Energy*, vol. 77, pp. 641–666, Dec. 2014, doi: 10.1016/j.energy.2014.09.063.
- [4] S. Nagai et al., “30.5 A GaN 3 \times 3 matrix converter chipset with Drive-by-Microwave technologies,” in *2014 IEEE International Solid-State Circuits Conference Digest of Technical Papers (ISSCC)*, Feb. 2014, pp. 494–495. doi: 10.1109/ISSCC.2014.6757527.
- [5] C. Kuring, J. Lenth, J. Boecker, T. Kahl, and S. Dieckerhoff, “Application of GaN-GITs in a Single-Phase T-Type Inverter,” in *PCIM Europe 2018; International Exhibition and Conference for Power Electronics, Intelligent Motion, Renewable Energy and Energy Management*, Jun. 2018, pp. 1–8. Accessed: Jul. 02, 2024. [Online]. Available: <https://ieeexplore.ieee.org/abstract/document/8402948>
- [6] M. Guacci, M. Tatic, D. Bortis, J. W. Kolar, Y. Kinoshita, and H. Ishida, “Novel Three-Phase Two-Third-Modulated Buck-Boost Current Source Inverter System Employing Dual-Gate Monolithic Bidirectional GaN e-FETs,” in *2019 IEEE 10th International Symposium on Power Electronics for Distributed Generation Systems (PEDG)*, Jun. 2019, pp. 674–683. doi: 10.1109/PEDG.2019.8807580.
- [7] J. Zhu, Q. Zeng, X. Yang, M. Zhou, and T. Wei, “A Bidirectional MVDC Solid-State Circuit Breaker Based on Mixture Device,” *IEEE Trans. Power Electron.*, vol. 37, no. 10, pp. 11486–11490, Oct. 2022, doi: 10.1109/TPEL.2022.3171805.
- [8] Z. J. Shen et al., “First experimental demonstration of solid state circuit breaker (SSCB) using 650V GaN-based monolithic bidirectional switch,” in *2016 28th International Symposium on Power Semiconductor Devices and ICs (ISPSD)*, Jun. 2016, pp. 79–82. doi: 10.1109/ISPSD.2016.7520782.

- [9] J. Waldron and T. P. Chow, "Physics-based analytical model for high-voltage bidirectional GaN transistors using lateral GaN power HEMT," in *2013 25th International Symposium on Power Semiconductor Devices & IC's (ISPSD)*, May 2013, pp. 213–216. doi: 10.1109/ISPSD.2013.6694483.
- [10] H. Wang et al., "Experimental Demonstration of Monolithic Bidirectional Switch With Anti-Paralleled Reverse Blocking p-GaN HEMTs," *IEEE Electron Device Letters*, vol. 42, no. 9, pp. 1264–1267, Sep. 2021, doi: 10.1109/LED.2021.3098040.
- [11] M. Saadeh, M. S. Chinthavali, B. Ozpineci, and H. A. Mantooth, "Anti-series normally-On SiC JFETs operating as bidirectional switches," in *2013 IEEE Energy Conversion Congress and Exposition*, Sep. 2013, pp. 2892–2897. doi: 10.1109/ECCE.2013.6647077.
- [12] Z. Wang, R. Sun, Z. Wang, and B. Zhang, "Reverse Blocking GaN High Electron Mobility Transistors with Stepped P-GaN Drain," *ECS J. Solid State Sci. Technol.*, vol. 11, no. 2, p. 025002, Feb. 2022, doi: 10.1149/2162-8777/ac5165.
- [13] J. Huber and J. W. Kolar, "Monolithic Bidirectional Power Transistors," *IEEE Power Electronics Magazine*, vol. 10, no. 1, pp. 28–38, Mar. 2023, doi: 10.1109/MPEL.2023.3234747.
- [14] T. Morita et al., "650 V 3.1 mΩcm² GaN-based monolithic bidirectional switch using normally-off gate injection transistor," in *2007 IEEE International Electron Devices Meeting*, Dec. 2007, pp. 865–868. doi: 10.1109/IEDM.2007.4419086.
- [15] U. Raheja et al., "Applications and characterization of four quadrant GaN switch," in *2017 IEEE Energy Conversion Congress and Exposition (ECCE)*, Oct. 2017, pp. 1967–1975. doi: 10.1109/ECCE.2017.8096397.
- [16] G. Gupta et al., "Innovations in GaN Four Quadrant Switch technology," in *2023 IEEE 10th Workshop on Wide Bandgap Power Devices & Applications (WiPDA)*, Dec. 2023, pp. 1–4. doi: 10.1109/WiPDA58524.2023.10382202.
- [17] S. Musumeci, M. Panizza, F. Stella, and F. Perraud, "Monolithic Bidirectional Switch Based on GaN Gate Injection Transistors," in *2020 IEEE 29th International Symposium on Industrial Electronics (ISIE)*, Jun. 2020, pp. 1045–1050. doi: 10.1109/ISIE45063.2020.9152230.
- [18] C. Kuring, O. Hilt, J. Böcker, M. Wolf, S. Dieckerhoff, and J. Würfl, "Novel monolithically integrated bidirectional GaN HEMT," in *2018 IEEE Energy Conversion Congress and Exposition (ECCE)*, Sep. 2018, pp. 876–883. doi: 10.1109/ECCE.2018.8557741.
- [19] M. Wolf, O. Hilt, and J. Würfl, "Gate Control Scheme of Monolithically Integrated Normally OFF Bidirectional 600-V GaN HFETs," *IEEE Transactions on Electron Devices*, vol. 65, no. 9, pp. 3878–3883, Sep. 2018, doi: 10.1109/TED.2018.2857848.
- [20] N. Nain, S. Walser, J. Huber, K. K. Leong, and J. W. Kolar, "Self-Reverse-Blocking Control of Dual-Gate Monolithic Bidirectional GaN Switch With Quasi-Ohmic on-State Characteristic," *IEEE Transactions on Power Electronics*, vol. 37, no. 9, pp. 10091–10094, Sep. 2022, doi: 10.1109/TPEL.2022.3163589.
- [21] C. Kuring et al., "Impact of Substrate Termination on Dynamic On-State Characteristics of a Normally-off Monolithically Integrated Bidirectional GaN HEMT," in *2019 IEEE Energy Conversion Congress and Exposition (ECCE)*, Sep. 2019, pp. 824–831. doi: 10.1109/ECCE.2019.8912793.
- [22] M. T. Alam, J. Chen, R. Bai, S. S. Pasayat, and C. Gupta, "High-Voltage (>1.2 kV) AlGaIn/GaN Monolithic Bidirectional HEMTs With Low On-Resistance (2.54 mΩ · cm²)," *IEEE Transactions on Electron Devices*, vol. 71, no. 1, Jan. 2024, doi: 10.1109/TED.2023.3330133.
- [23] G. Greco, F. Iucolano, and F. Roccaforte, "Review of technology for normally-off HEMTs with p-GaN gate," *Materials Science in Semiconductor Processing*, vol. 78, pp. 96–106, May 2018, doi: 10.1016/j.mssp.2017.09.027.
- [24] F. Roccaforte, G. Greco, P. Fiorenza, and F. Iucolano, "An Overview of Normally-Off GaN-Based High Electron Mobility Transistors," *Materials*, vol. 12, no. 10, Art. no. 10, Jan. 2019, doi: 10.3390/ma12101599.
- [25] X. Huang, Z. Liu, Q. Li, and F. C. Lee, "Evaluation and Application of 600 V GaN HEMT in Cascode Structure," *IEEE Transactions on Power Electronics*, vol. 29, no. 5, pp. 2453–2461, May 2014, doi: 10.1109/TPEL.2013.2276127.
- [26] T. Hirose et al., "Dynamic performances of GaN-HEMT on Si in cascode configuration," in *2014 IEEE Applied Power Electronics Conference and Exposition - APEC 2014*, Mar. 2014, pp. 174–181. doi: 10.1109/APEC.2014.6803306.
- [27] D. Bisi et al., "Short-Circuit Capability with GaN HEMTs: Invited," in *2022 IEEE International Reliability Physics Symposium (IRPS)*, Mar. 2022, pp. 1–7. doi: 10.1109/IRPS48227.2022.9764492.
- [28] D. Bisi et al., "Short-Circuit Protection for GaN Power Devices with Integrated Current Limiter and Commercial Gate Driver," in *2022 IEEE Applied Power Electronics Conference and Exposition (APEC)*, Mar. 2022, pp. 181–185. doi: 10.1109/APEC43599.2022.9773446.
- [29] G. Gupta et al., "1200V GaN Switches on Sapphire Substrate," in *2022 IEEE 34th International Symposium on Power Semiconductor Devices and ICs (ISPSD)*, May 2022, pp. 349–352. doi: 10.1109/ISPSD49238.2022.9813640.
- [30] G. Gupta et al., "1200V GaN Switches on Sapphire: A low-cost, high-performance platform for EV and industrial applications," in *2022 International Electron Devices Meeting (IEDM)*, Dec. 2022, p. 35.2.1–35.2.4. doi: 10.1109/IEDM45625.2022.10019381.
- [31] X. Li et al., "1700 V High-Performance GaN HEMTs on 6-inch Sapphire With 1.5 μm Thin Buffer," *IEEE Electron Device Letters*, vol. 45, no. 1, pp. 84–87, Jan. 2024, doi: 10.1109/LED.2023.3335393.
- [32] T. P. Chuang, N. Tumilty, C. H. Yu, and R. H. Horng, "Comparison of performance in GaN-HEMTs on thin SiC substrate and Sapphire substrates," *Chinese Journal of Physics*, Jun. 2024, doi: 10.1016/j.cjph.2024.06.011.
- [33] J.-G. Kim, C. Cho, E. Kim, J. S. Hwang, K.-H. Park, and J.-H. Lee, "High Breakdown Voltage and Low-Current Dispersion in AlGaIn/GaN HEMTs With High-Quality AlN Buffer Layer," *IEEE Transactions on Electron Devices*, vol. 68, no. 4, pp. 1513–1517, Apr. 2021, doi: 10.1109/TED.2021.3057000.
- [34] C. Yu et al., "High Voltage Normally-Off p-GaN Gate HEMT with the Compatible High Threshold and Drain Current," *ECS J. Solid State Sci. Technol.*, vol. 11, no. 8, p. 085009, Aug. 2022, doi: 10.1149/2162-8777/ac8a71.
- [35] B. Duan, L. Yang, Y. Wang, and Y. Yang, "Experimental Results for AlGaIn/GaN HEMTs Improving Breakdown Voltage and Output Current by Electric Field Modulation," *IEEE Transactions on Electron Devices*, vol. 68, no. 5, pp. 2240–2245, May 2021, doi: 10.1109/TED.2021.3067865.